Research Square

Preprints are preliminary reports that have not undergone peer review.
They should not be considered conclusive, used to inform clinical practice,
or referenced by the media as validated information.

Numerical simulation and experimental investigation on edge qualities of blanked surface characteristics under ultra-high-speed blanking

mohamed sahli

mohamed.sahli@unicaen.fr

CIMAP: Centre de recherche sur les ions les materiaux et la photonique https://orcid.org/0000-0002-8690-5366

Faleh Rabhi

Rofka Ramdani

Mohamed Abid

Research Article

Keywords: Metal blanking, shear surface, plastic forming, numerical simulation, steel sheet, finite element method (FEM)

Posted Date: June 25th, 2026

DOI: https://doi.org/10.21203/rs.3.rs-9612213/v1

License: This work is licensed under a Creative Commons Attribution 4.0 International License.
Read Full License

Numerical simulation and experimental investigation on edge qualities of blanked surface characteristics under ultra-high-speed blanking

Mohamed Sahli[1,a], Faleh Rabhi[2], Rofka Ramdani[3], Mohamed Abid[4]

[1]Normandie Univ, ENSICAEN, UNICAEN, CEA, CNRS, CIMAP, 14000 Caen, France
[2]Univ. Bourgogne Franche-Comté, Femto-ST Institute, CNRS/UFC/ENSMM/UTBM, Department of Applied Mechanics, 25000 Besançon, France

[3]Université Bourgogne Europe, CNRS, Laboratoire Interdisciplinaire Carnot de Bourgogne ICB UMR 6303, 71200 Le Creusot, France
mohamed.sahli@unicaen.fr

Abstract: Metal blanking was a widely used process in the manufacture of metal components for the automotive, aerospace, and civil engineering industries. This process involves cutting metal using a rigid punch and die with a mechanical or hydraulic press. Shearing occurs through the gap between the punch and the die, resulting in the complete rupture of the sheet metal. Optimizing the final shape of the produced metal parts relies primarily on a thorough understanding of this shearing process. This article presents the results of studies, combining numerical calculations and experimental verification, focusing on the influence of certain parameters of the blanking process on the stress state of cold-rolled steel sheets.

Numerical simulation models for blanking 16MnCr5 steel parts were developed using the commercial software Lsdyna to analyze the influence of various parameters on the quality of the fracture surface, including die gaps and the effect of heating due to cutting tool friction. Mechanical tests and experimental characterization of the sheet metal were performed to adjust the parameters of the constitutive model to the experimental data and ultimately establish the appropriate constitutive law for the metal. This identified constitutive law was then used to run numerical simulations using LsDyna/Explicit software, covering various cutting tests.

It was observed that the quality of the cutting and the cut surface, based on a comparison of experimental results and numerical analysis, depends significantly on the gap between the punch and the die. Furthermore, a temperature rise occurs in both the sheet metal and the tooling due to the dissipation of a large portion of the plastic energy during cutting. Based on these results, a finite element model of the blanking process, capable of predicting surface defects, was developed.

Keywords: Metal blanking, shear surface, plastic forming, numerical simulation, steel sheet, finite element method (FEM)

1. Introduction

The sheet metal blanking was a process for shaping metal sheets with high precision and plays an important role in several industrial sectors. It was widely used for manufacturing metal parts primarily for the automotive and civil engineering industries [1-4]. It was also used for the mass production of parts for common household appliances [5,6]. sheet metal blanking was a classic elastoplastic deformation process. It can be divided into three main phases with fundamentally different physical behaviors [7]. The first phase was elastic deformation. After the punch makes contact with the sheet metal, the punch compresses it, and the sheet metal undergoes elastic deformation by compression. As the punch penetrates the material, it reaches its elastic limit and begins plastic deformation, which constitutes the second phase. This phase begins when the stresses in the deformation zone increase until they reach the material's elastic limit. In this phase, the extrusion depth of the sheet metal gradually increases, while the tensile stresses and bending moment in the material continue to increase. The material in the deformation zone undergoes work hardening. Then, the punch continues its penetration until cracks appear in the sheet metal near the cutting edges. When the cracks appear, this phase ends and the third phase, namely separation by rupture, begins. The punch continues to penetrate the sheet metal again and again, and the cracks near the cutting edges of the punch and die enlarge and propagate through the material. When the upper and lower cracks meet, the sheet metal breaks. The geometry of the tools and the parameters of the forming process clearly define the final shape and the quality of the surface finish of the cut edges of the finished product after the cutting phase. It was also essential to know that an incorrect design of the tools and the blank shape, or an inappropriate choice of material and process parameters, can result in a product with a non-conforming shape or defects.

Several studies mention that in the blanking process, the gap between the punch and the die influences not only the edge quality but also the force-displacement dynamics during the process [8,9]. For example, in the study conducted by Rachik et al. in 2002, they observed a slight decrease in cutting force when using increased punch-die gaps, while Mucha (2010) and Shivpuri et al. (2011) noted greater tool wear when using larger punch-die gaps [10-12]. Husson et al. (2008) observed that the quality of sheared edges was lower when using large punch/die gaps [13]. The same observation applies to tool wear, which was greater with larger gaps. As shown by Bratus et al. (2010), optimizing

the final shape of the edges of the cut part therefore involves using minimal clearance, which leads to improved geometric accuracy of the cut part [14]. Indeed, during sheet metal blanking, the material was subjected to various mechanical stresses. Under the effect of these stresses, the material undergoes significant elastic and plastic deformations, even leading to crack formation and complete material separation. Most of the energy was used for the macroscopic plastic deformation of the sheet metal. Up to 95% of the plastic deformation energy was converted into heat [15], and only a small fraction was stored in the material structure [16]. Thus, the dissipation of inelastic deformation energy causes a significant temperature rise in the shear zone, as well as at the punch and die. It was therefore essential to understand in detail the heat generation and its impact on the sheet metal blanking process, edge quality, and surface finish of the parts being cut.

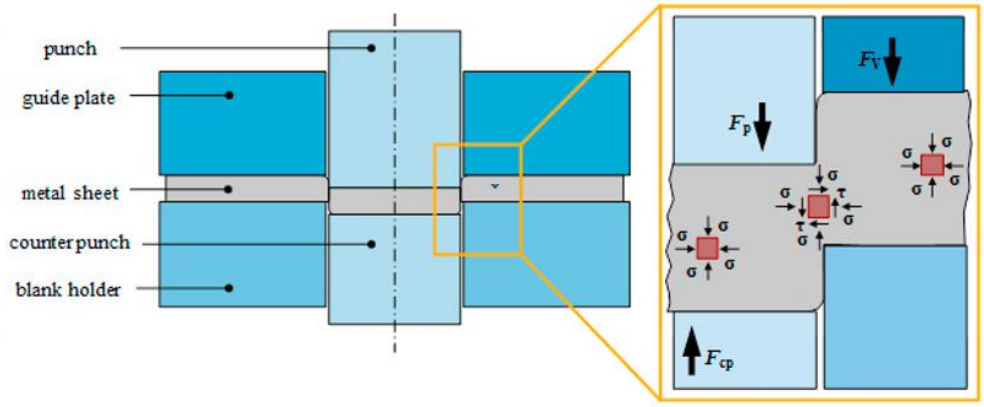


Fig. 1. Principle of blanking and hydrostatic compressive stress state in the shearing zone with punch force (F_p), counter punch force (F_{CP}) and Ring force (F_v) [17].

In recent years, thanks to increased numerical computing power, numerous analyses using various methods, primarily finite element analysis, have led to a better understanding of the mechanisms and phenomena involved in the blanking process [18-21]. Furthermore, numerical simulations of the blanking process using the finite element method are now a highly effective way not only to achieve cost savings and accelerate industrial production, but also to predict with sufficient accuracy the quality of the final cut profile of the cut parts. Recently, scientific studies on the sheet metal blanking process have been conducted using the finite element method [21-23]. Lind et al. (2010) found that the wear mechanism during cutting was characterized by three distinct phases: abrasive wear, adhesive wear, and the growth of friction zones [24]. Hogmark et al. (1981) also studied the wear behavior of punches following the cutting of steel sheets of different grades [25]. Their study concluded

that the material properties of the workpiece strongly influence the wear profile of the punches. Hemandez et al. (2006) sought to determine the optimal clearance by presenting the crack propagation angles along the shear edge [26]. Hambli et al. (2001) studied the same concept and also integrated neural networks to predict the burr height and optimize the blanking process [19]. Goijaerts et al. (2002) investigated this phenomenon and found that the maximum cutting force decreased due to thermal softening of the material [27]. Mori et al. (2012) demonstrated experimentally that the maximum cutting force decreased with preheating of the parts near the shear zone. Heat generation in the shear zone during the blanking process has been analyzed in various scientific studies using numerical simulations, for example in [28]. Zhang et al. (2015) also studied thermal cutting technology using Deforming-3D software [29]. The results showed that hot cutting forces and the cutting force of high-strength steel were significantly lower than those of cold cutting (early production). They also found that the quality of the cut area was better and die wear was reduced due to the generated heat. Peng et al. (2004) demonstrated numerically that a reduction of approximately 75% in the maximum force could be achieved simply through preheating [30]. Sartkulvanich et al. (2010), meanwhile, observed minor variations in cutting force due to temperature in the shear zone [31].

In this article, we propose a finite element analysis (FEM) of the blanking process, using different punch-die clearances. The objective of this work was to establish a reliable model using 2D axisymmetric FE simulation to study the influence of the punch-die clearance and the progressive heating of the punch on the dimensional quality and surface finish of the parts obtained by cutting. From a global perspective, this study aims to predict the distribution of shear stresses and plastic strains in the shear zone during cutting, as a function of the punch-die clearance (J), at different temperatures, and to study their influence on the quality of the cutting edge. An attempt to validate the proposed numerical model will be presented in terms of comparing the cutting forces and the profiles of the sheared edges with appropriate experimental analysis.

2. Material and experimental method

2.1. Material

In the blanking process, a 16MnCr5 steel coil was used as the cutting material. Its mechanical properties are listed in Table 1. Tensile tests were performed using an Instron servo-electric machine with a maximum load capacity of 100 kN, with an accuracy of 0.2% for the force sensor (resolution of 0.01 N) and an accuracy of 0.06% for the displacement

sensor (resolution of 0.001 mm). The tensile testing apparatus, equipped with an online strain measurement system, was shown in Fig.2. Table 2 presents the chemical composition and Table 1 the associated mechanical properties of the metallic material used in this study. The tensile strength was estimated at approximately 450 MPa for an elongation of 36%.

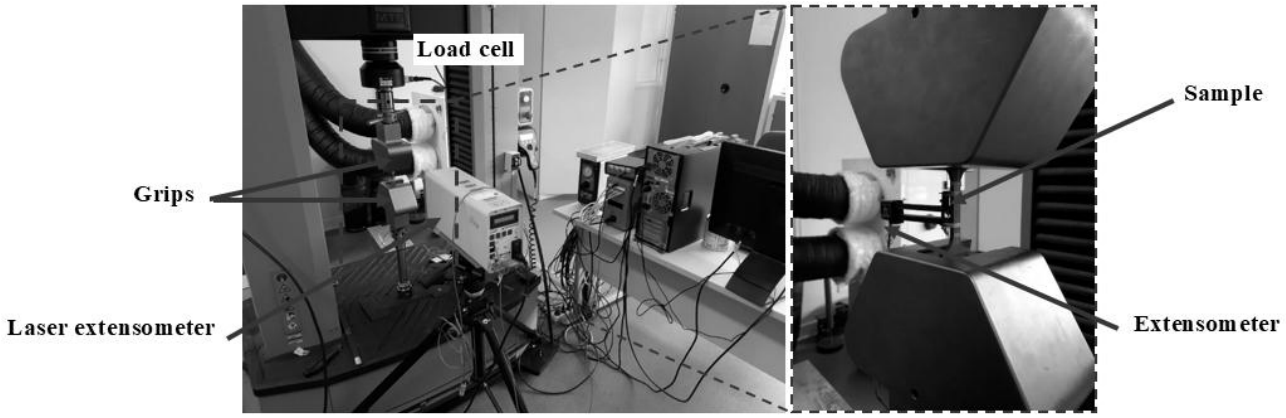


Fig. 2. Experimental setup for tensile testing using servo-electric Instron test.

Figure 3a shows the stress-strain curves of all the samples. In this study, the slope of the stress-strain curve in the elastic phase was defined as the initial modulus of elasticity.
Flat tensile test specimens were cut so that the loading axis was aligned with the rolling direction of the sheet and/or perpendicular to it. A constant strain rate of 1 mm/s was imposed during the tensile test. All tests were carried out until the tensile specimens failed (see Fig.3a). The stress-strain curves of these subjected specimens are shown in Figure 3b. It was observed that the rolling direction induces a preferred crystallographic orientation in the microstructure, which gives the sheet superior mechanical strength. Consequently, the mechanical properties tend to be weaker in the transverse direction, i.e., perpendicular to the rolling direction. All of these experimental data were integrated into simulation codes to describe the behavior of the steel sheet (see Table 1).

Tensile strength R_m	Yield strength $R_{0.2}$	Young's modulus	Poisson's ratio
453 MPa	348 MPa	211 GPa	0.32

Table 1. Material properties of the 16MnCr5 sheet.

C	Mn	Si	S	P	Cr
0.13-0.18	1.1-1.3	0.40	0.032	0.035	0.79-1.10

Table 2. Chemical composition (average), [%].

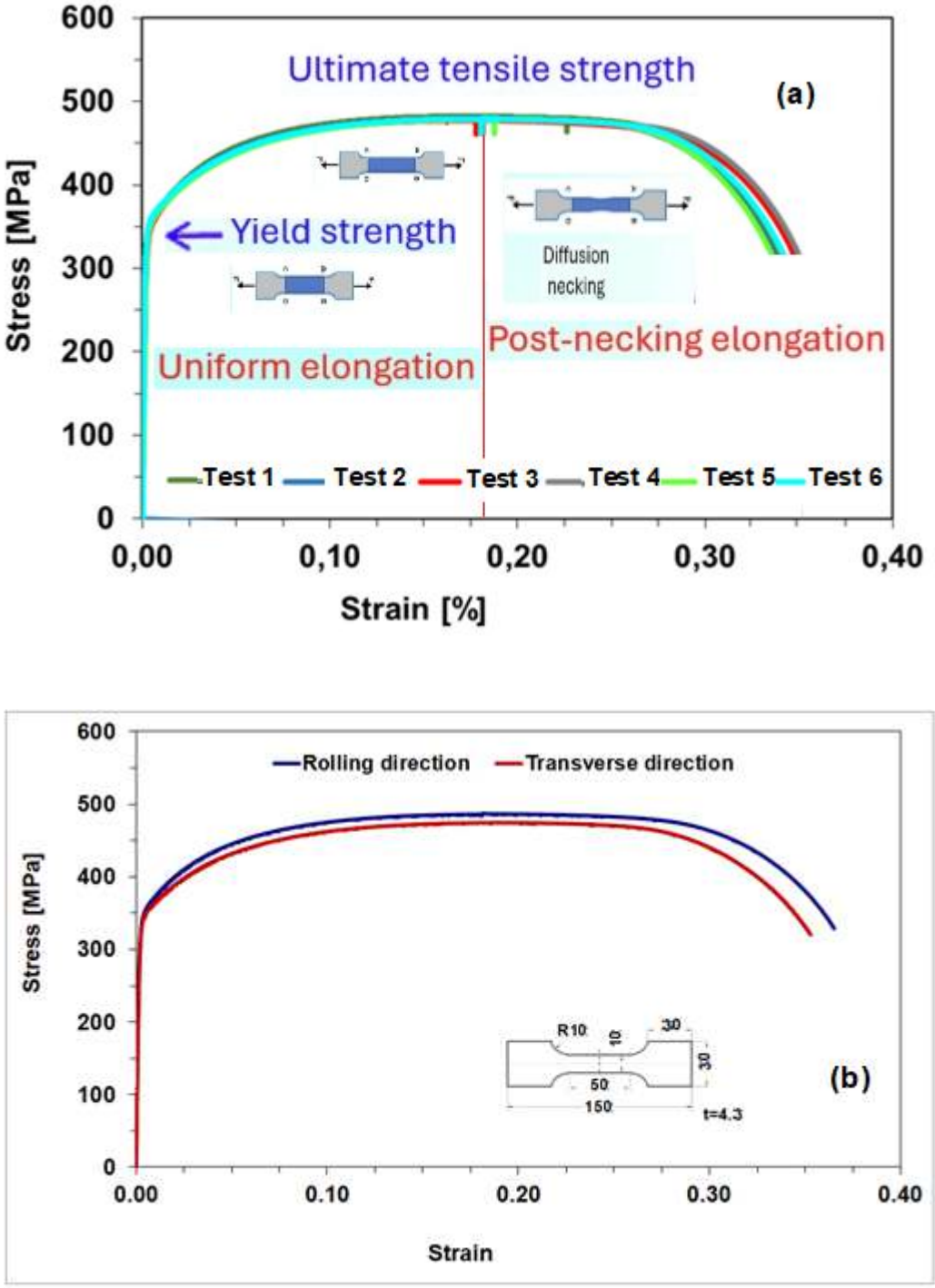


Fig. 3. Stress-strain relationship of 16MnCr5.

The data collected concerning the mechanical properties obtained through tensile testing include yield strength, tensile strength, uniform elongation, and total elongation. The distribution of tensile properties was illustrated by the histograms in Fig.4. It was noteworthy that the four histograms show that the data obtained vary little between the different sheets tested and were quite close to those reported in the literature. They follow a normal distribution.

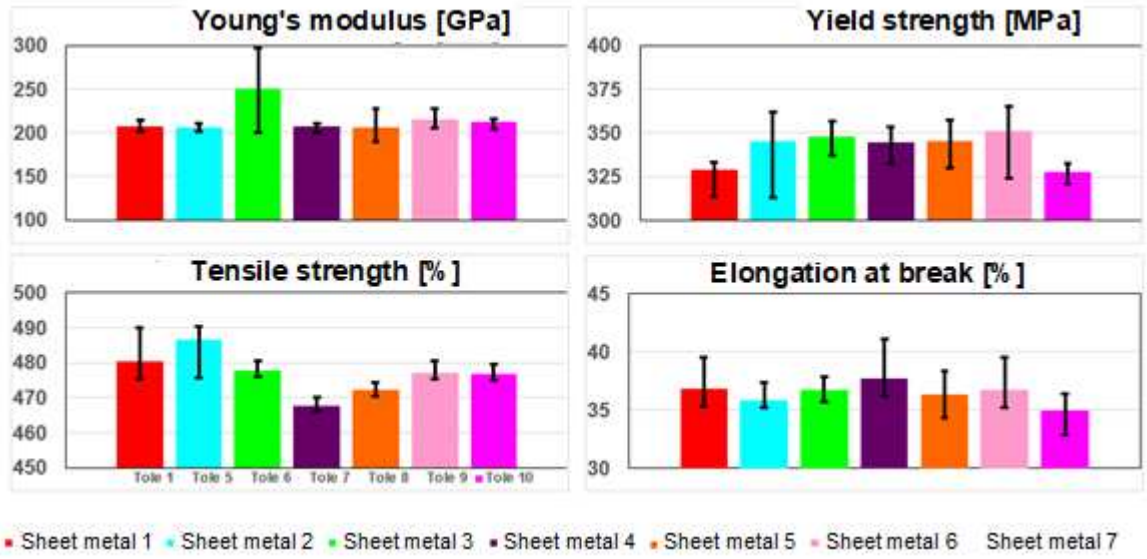


Fig.4. Histogram of tensile properties.

All tests were continued until the sample broke. High-magnification microscopic observations were made on the fracture zones of the tensile specimens to determine the mode of failure, as illustrated in Fig.5. The observed fracture was entirely ductile with a dull appearance.

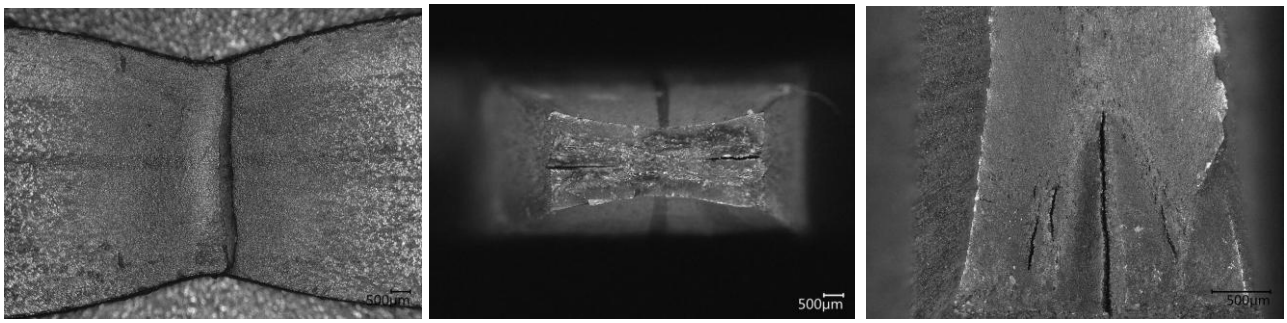


Fig.5. Optical microscopic structure of necking.

2.2. Blanking test description

The cutting tests were performed on a hydraulic press at a speed of 20 strokes/min. Several sensors were used to instrument the cutting tool to monitor important process data during the various cutting operations. Piezoelectric sensor pads dedicated to acquiring the punching force and a length gauge were used to accurately measure the punch stroke during the cutting cycle. To obtain an absolute temperature value, three calibrated temperature sensors were placed in different areas of the tooling. The system was controlled by a LABVIEW® program. The displacement/temperature signals recorded during a cut are shown in Figs.7 and 8. The instrumented tooling was designed to perform a cutting operation on a metal part from a 4.2 mm thick sheet metal strip with a cycle time of 1.5 s (see

Fig.7). The punch stroke was adjusted to achieve a penetration depth of 5.8 mm, with the actual cutting time approximately 0.4 s. In this study, four sets of parameters were used for the punch/stripper (J1) and the punch/die (J2): (J1/J2) equals (0.1/0.01), (0.1/0.1), and (0.01/0.1), see Fig.6.

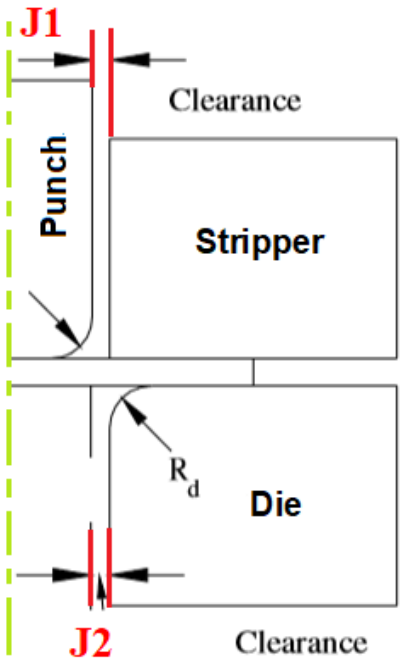


Fig. 6. Geometry of punch, die, stripper, metal sheet and clearance.

A temperature measurement system based on three thermocouples was integrated into the cutting tool, as close as possible to the punch. Temperature profiles were recorded for identical punch displacements and an identical punch/die clearance of 0.1 mm. The heat generation during cutting, represented by the measured temperature profiles, exhibits similar characteristics regardless of the measurement point (see Fig.7). A sharp temperature increase was observed up to 875 cycles. Thereafter, a slight temperature rise was detected despite heat dissipation in adjacent areas. Finally, the temperature stabilizes around 50±2°C from 4500 cycles onward. Four temperatures were selected for our numerical simulations to predict the distribution of shear stresses and plastic strains in the shear zone. The vertical displacement of the tool as a function of cycle time, obtained from instrumented cutting tests, was illustrated in Fig.8.

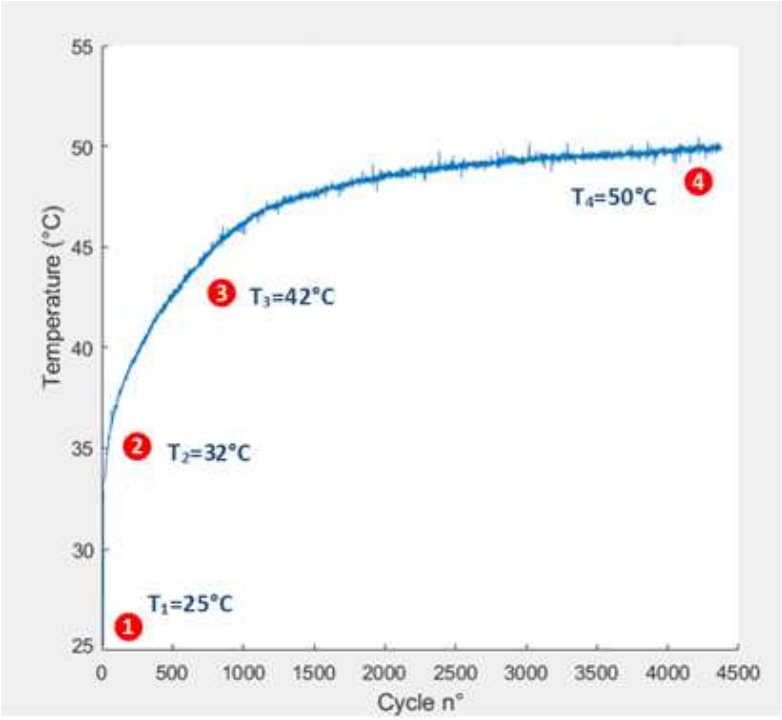


Fig.7. Averaged temperatures of the rigid punch surface during blanking test.

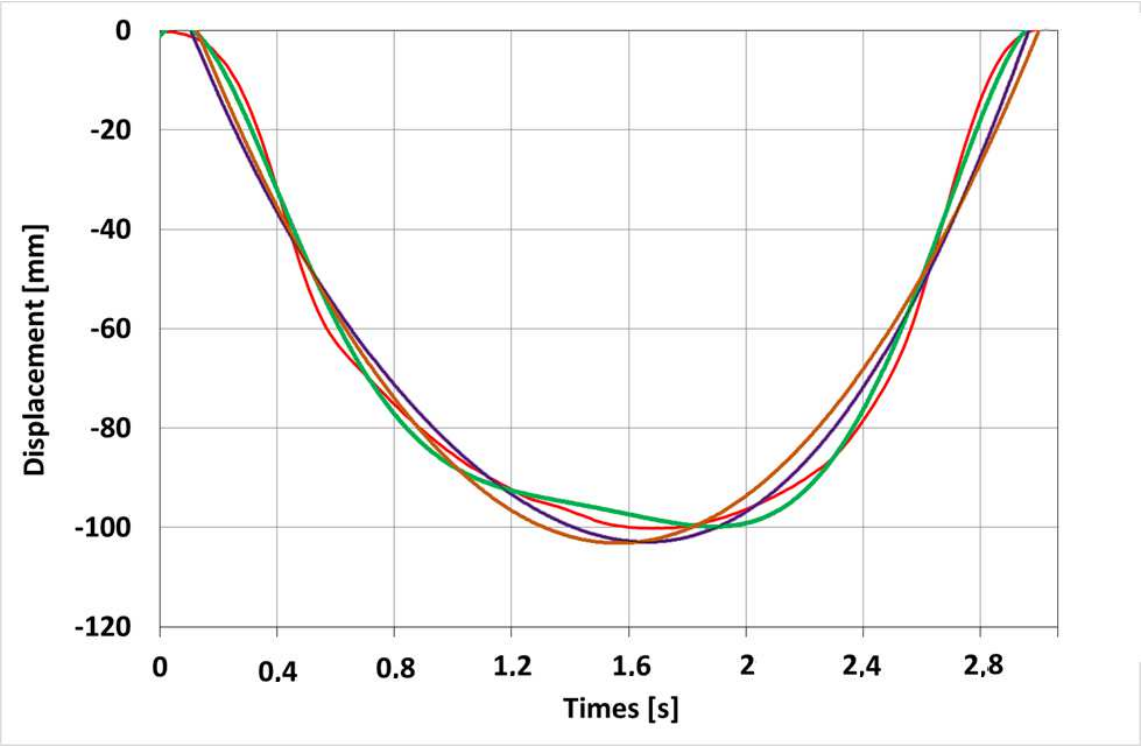
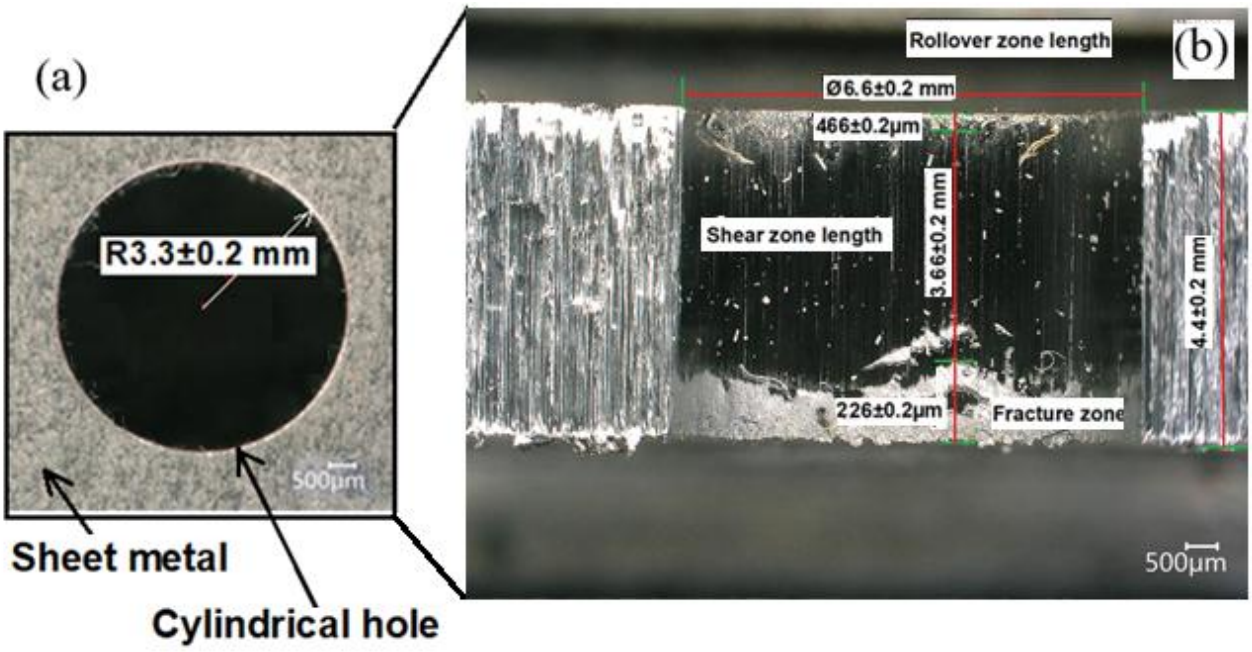


Fig.8. Signals measured during blanking test.

Microstructural analysis was performed using a Keyence Co., Ltd. (Japan) digital microscope to evaluate the surface condition of the edges after cutting, using various die-punch clearances. Figure 9 shows a macrophotograph of sections of an area cut with a 6.6 mm diameter cylindrical punch. They show microscopic views of the edge of a hole obtained on a cylindrical hole made by blanking process. Note the depth of burnished and

fracture in the right images (see Fig.9b), as well as the microcracks and burrs in Fig.10b. It highlights the presence of different edge zones: rollover, burnished, fractured, and burr. The magnification of the area near the sheared or burnished cutting edge illustrates the degree of microstructural deformation. The depth of the sheared zone was approximately 3.55 ± 0.2 mm, which corresponds to more than half the sheet thickness, averaged values and presented in Fig.9. It was observed that the depth of the rollover/fractured zones was significantly affected by the punch-die clearance. It tends to decrease for smaller values of this clearance in the cutting tool.

Consequently, the final surfaces obtained by blanking process frequently exhibit very significant defects and disadvantages such as significant deformations and large defects on the sheared edge, such as burrs and edge undulations (Fig.10b).



J1/J2=0.1/0.01

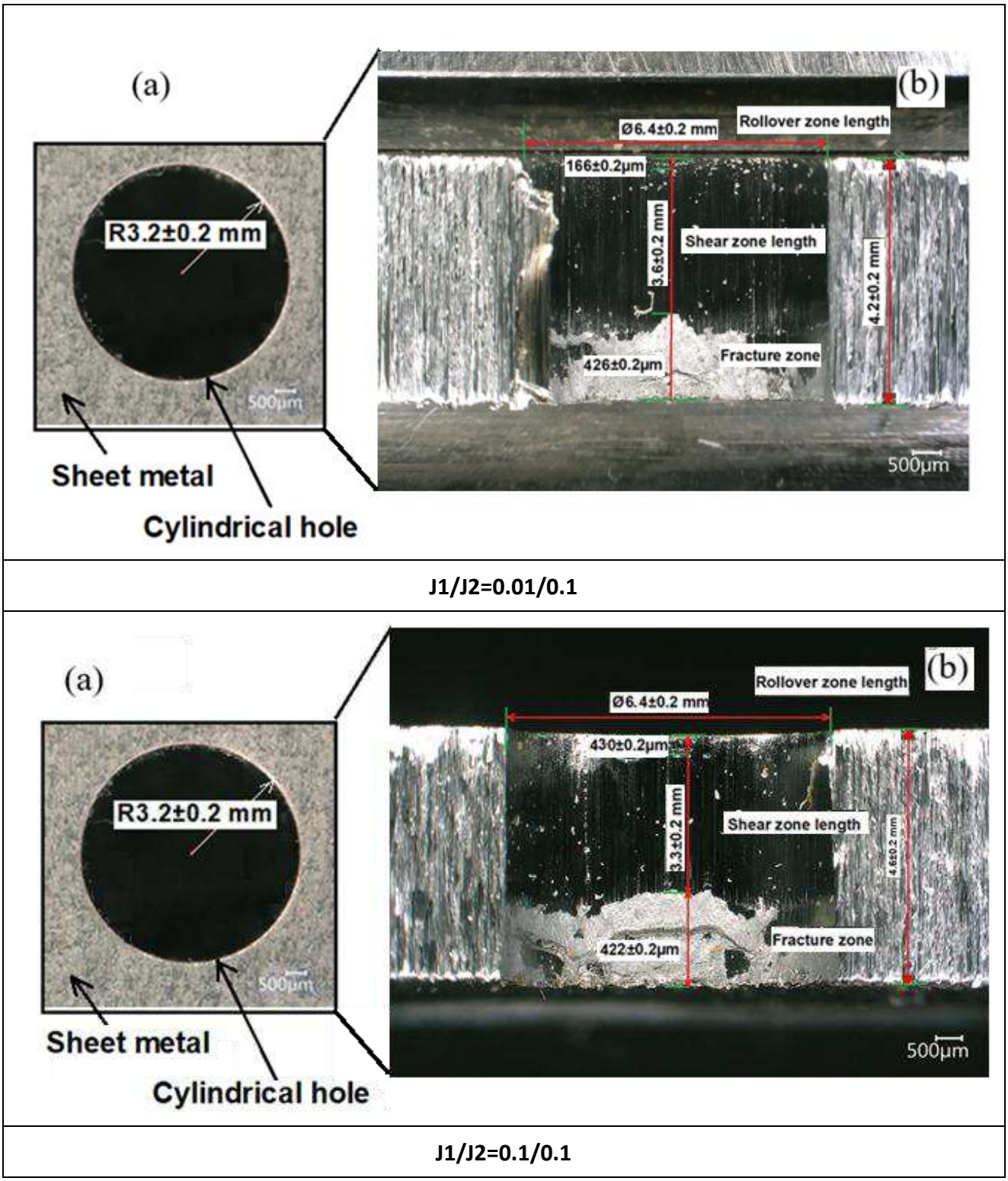


Fig.9. (a) Blanking process of sheet metal: (a) sheet metal with cylindrical hole, and (b) cross-sections of sample.

The image clearly illustrates the secondary burnish formation in highly variable proportions. These range from subtle secondary burnish to strongly manifested that blend seamlessly with primary burnish. Some irregular burrs and rough cut-edge fracture surfaces were also visible (see Fig.10).

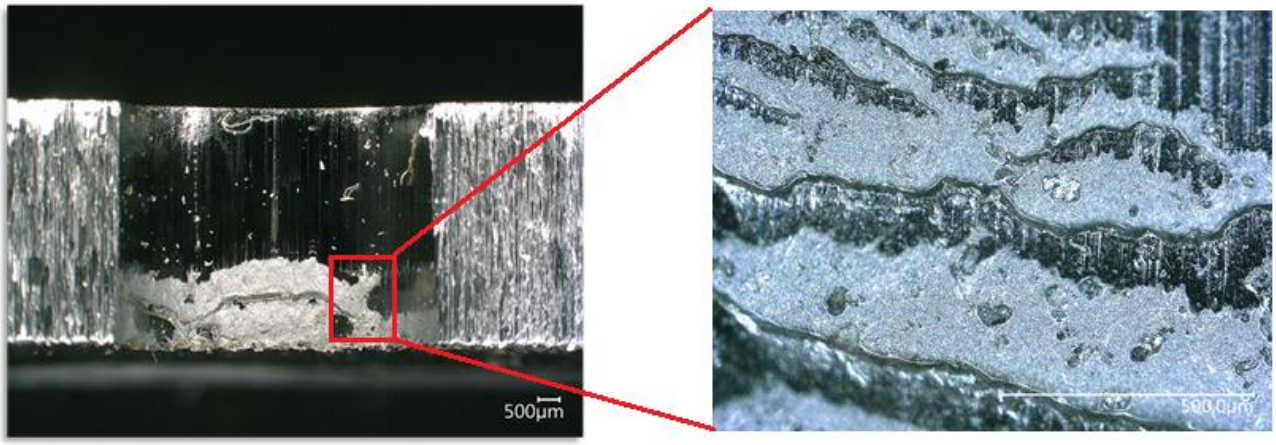


Fig.10. Panoramic cut edges obtained using a cylindrical punch, showing the formation of secondary burnishing and the formation of complete and partial burrs on steel sheets.

3. Finite element modelling of the blanking process

3.1. Sheet metal material behaviour modelling

The elastoplastic behavior of the sheet metal has been described by a Johnson-Cook plasticity model whose parameters remain to be identified and validated through tensile tests [32].

$$\sigma = (A + B\varepsilon^n)\left[1 + C\ln\left(\frac{\dot{\varepsilon}}{\dot{\varepsilon}_0}\right)\right]\left[1 - \left(\frac{T - T_r}{T_m - T_r}\right)^m\right]$$

In this equation, *A, B* and C are the initial yield stress, strain hardening coefficient and reference strain rate coefficient, n was the strain hardening exponent, $\dot{\varepsilon_p}$ was the rate of plastic strain. The thermal softening parameter was denoted by *m*. The Johnson-Cook model parameters for 16MnCr5, which were listed in Table 3.

The fitness function of the genetic algorithm was obtained from the least squares principle as follows [33]:

$$(A, B, n, C, m) = k_1\left(\sum_{i=1}^{N}\left[\frac{A + B\varepsilon_{AB}^n(i)}{\sigma_{AB}}\left(1 + C\ln\left(\frac{\dot{\varepsilon}_{AB}(i)}{\dot{\varepsilon}_0}\right)\right)\left(1 - \left(\frac{T_{AB}(i) - T_r}{T_m - T_r}\right)^m\right) - 1\right]^2\right)$$

N represents the experimental groups number, k1 refers to a proportionality constant value -1 and i expresses the experimental sequence number.

Table 3. Johnson-Cook strength model parameters for **16MnCr5**.

Parameters	Values
	16MnCr5
Initial Yield Stress A	239
Hardening Constant B	522
Hardening exponent N	0.65
Strain Rate Constant C	0.02
Thermal Softening Exponent m	1
Reference Strain Rate (/sec)	1

At the end of the identification process, a set of parameters was determined and then validated through a comparative study between tensile tests and the modeling of the constitutive laws used in this study (see table 3). For monotonic tensile loadings, both experimental and modeling approaches provide fairly similar responses in terms of stress evolution versus function of strain, with better prediction in the elastic part with a maximum average gap of 8.3% (see Fig.11). On the elastic part the model was perfectly accurate with respect to the experimental data. Some discrepancies were observed at the beginning of the inelastic behaviour. However, we can therefore admit that these results were valid.

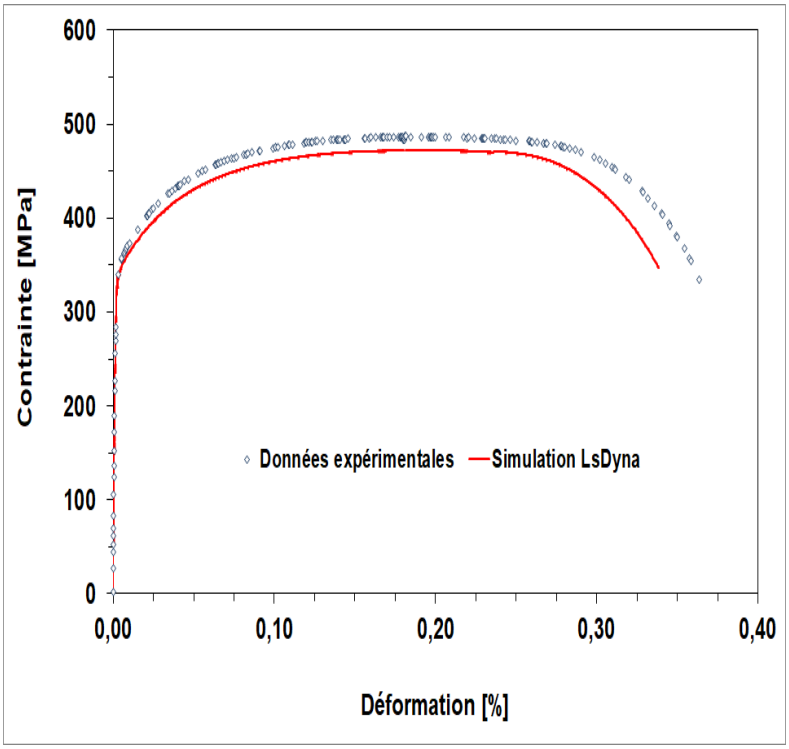


Fig.11. Comparison of results between experimental and simulation at room temperature in the rolling direction of a DP steel specimen.

3.2. Finite element model and process parameters

The finite element (FE) analysis of the blanking process was performed using the commercial software LS-DYNA. The cutting operation was modeled in a 2D axisymmetric configuration. Figure 12 illustrates an overview of the modeled tooling setup, and Table 4 lists the model input parameters. The finite element simulation was performed with a rigid, non-deformable punch under a constant imposed displacement. Different punch-die clearances were tested to study their influence on the final quality of the cut edges. The total mesh comprised approximately 6.653 elements, including 25 elements within the sheet thickness. For reference, the part to be cut was meshed with PLANE183 elements with reduced integration. In this study, the mesh regenerates adaptively as a function of plastic deformation. The lower die, the punch, and the blank holder were considered rigid, undeformable bodies, while the cut sheet metal was modeled as a deformable isotropic elastoplastic material. The initial sheet metal thickness was 4.6 mm. The exponential hardening law of the sheet metal was determined by tensile tests. Poisson's ratio was 0.3, and the Young's modulus was 210 GPa for all sheets.

In the absence of information on the temperature evolution within the tooling during cutting, it was reasonable to consider the heat transfer coefficient (HTC) as constant in the numerical simulations to predict the temperature evolution of the cutting tool during the process. The heating of the punch during cutting was simulated at different temperatures. Its boundary conditions were defined as shown in Fig.12, and the input parameters were presented in Table 5. For contact friction, surface-to-surface contacts between the tool and the workpiece were defined. A Coulomb coefficient of friction of 0.1 was used for all contacts.

N°	Name of the part	Kind of Part	Initial number of Nodes	Initial number of Elements
1	Punch	Rigid	1209	1140
2	Stipper	Deformable	616	569
3	Workpiece	Elasto-plastic	4576	4375
4	Die	Rigid	616	569
			Total Number: 7017/6653	

Table 4. FEM simulation conditions.

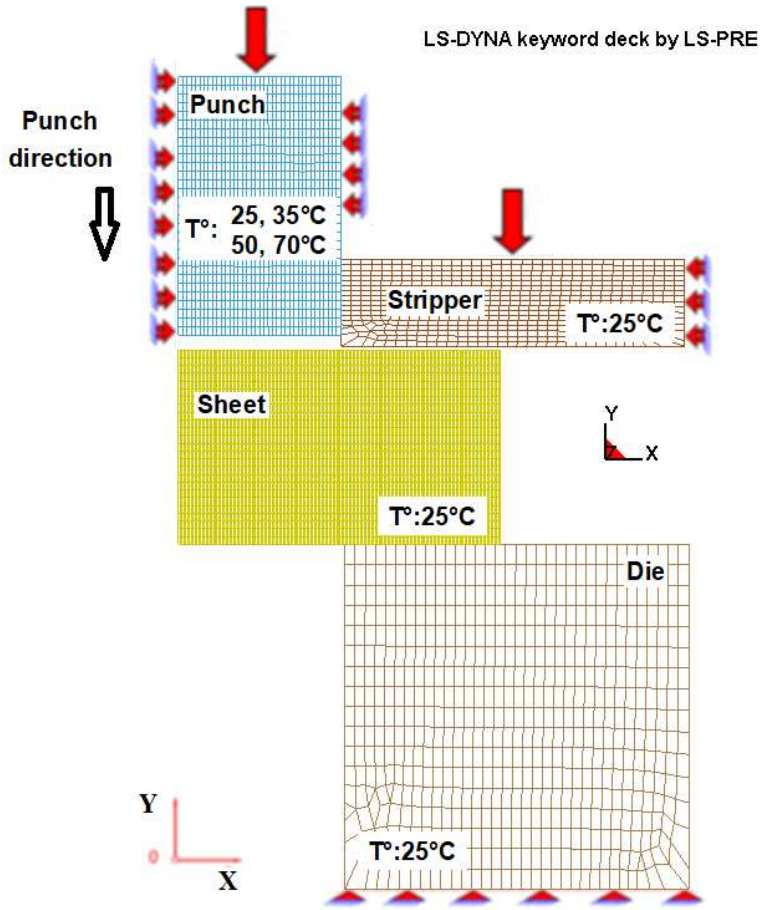


Fig.12. Axisymmetric blanking simulation scheme.

	Punch	Stipper	Workpiece	Die
Initial temperature (°C)	25-35-50-70	25	25	25
Heat capacity (J/(kg·K))	460	460	460	460
Heat transfer coefficient HTC (kW/(m²·K))	46	46	46	46
Coefficient of friction	0.1	0.1	0.1	0.1
Clearances punch/die (mm)	0.1	-	-	0.1
Clearances punch/stripper (mm)	0.01	0.01	-	-

Table 5. Input parameters for numerical simulation.

4. Numerical results of the blanking test

A comparison of effective plastic strain distribution with or without thermal coupling in blanking process, was shown in Fig.13. With the increase of punch penetration in the sheet, cracks simultaneously initiate under the punch corner radius and over the die corner radius. Then the cracks propagate along a straight line connecting both cracks. The consideration of thermal coupling leads to low decreasing of tensile stresses and less pronounced estimated between 1% to 2% with increasing of plastic strain values between 2.5 to 4.3% in shearing zone. This behavior was physically reasonable, compressive stresses delay then the evolution of damage. These numerically obtained results agree well with a experimental

study of Demmel et al. (2015) [34]. The localization of plastic deformation to material areas nearby the cutting edge of the punch effects a rapid heat generation and therefore a progressive temperature rise (see Fig.14).

In our FE model, the thermomechanical coupling was determined based on experimental observations. After a few cycles, the components of our tooling will rise from ambient temperature to 50°C due to repeated friction between them. Indeed, the punch reaches this temperature after a certain number of cutting cycles. This often leads to the cutting operation being performed under conditions where the sheet metal/die was at 25°C and the punch was at 50°C.

The initial results were shown in Fig.14. It illustrates the temperature evolution through the sheet metal thickness, i.e., in the shear zone induced by the cutting operation, and also on the adjacent surface of the punch/blank holder during a cutting cycle. As this figure clearly shows, the sheet metal temperature gradually increases and reaches a high value of 50°C. It was clear that the stress state in the shear zone will be different at 50°C (after a certain number of shearing cycles) than at 25°C (first shearing cycles). This result was consistent with experimental findings. Rafsanjani et al. (2009) also demonstrated numerically that the temperature in the shear zone increases until failure and then decreases rapidly; however, outside this zone, the temperature continues to rise [35].

Several simulations were performed to study the temperature evolution within the tooling during a cycle in the blanking process. Simulations were conducted at ambient temperature, corresponding to the start of the process; then at 42°C, corresponding to approximately ten cutting cycles; and finally at 50°C, the maximum temperature experimentally recorded during a production day (see Fig.15). Indeed, the heat generated by the regular friction between the punch and the sheet metal during cutting propagates very rapidly via the classic process of thermal conduction to adjacent areas of the material. It was sensitive to the gap between the punch and the die, as it increases more rapidly as the gap decreases.

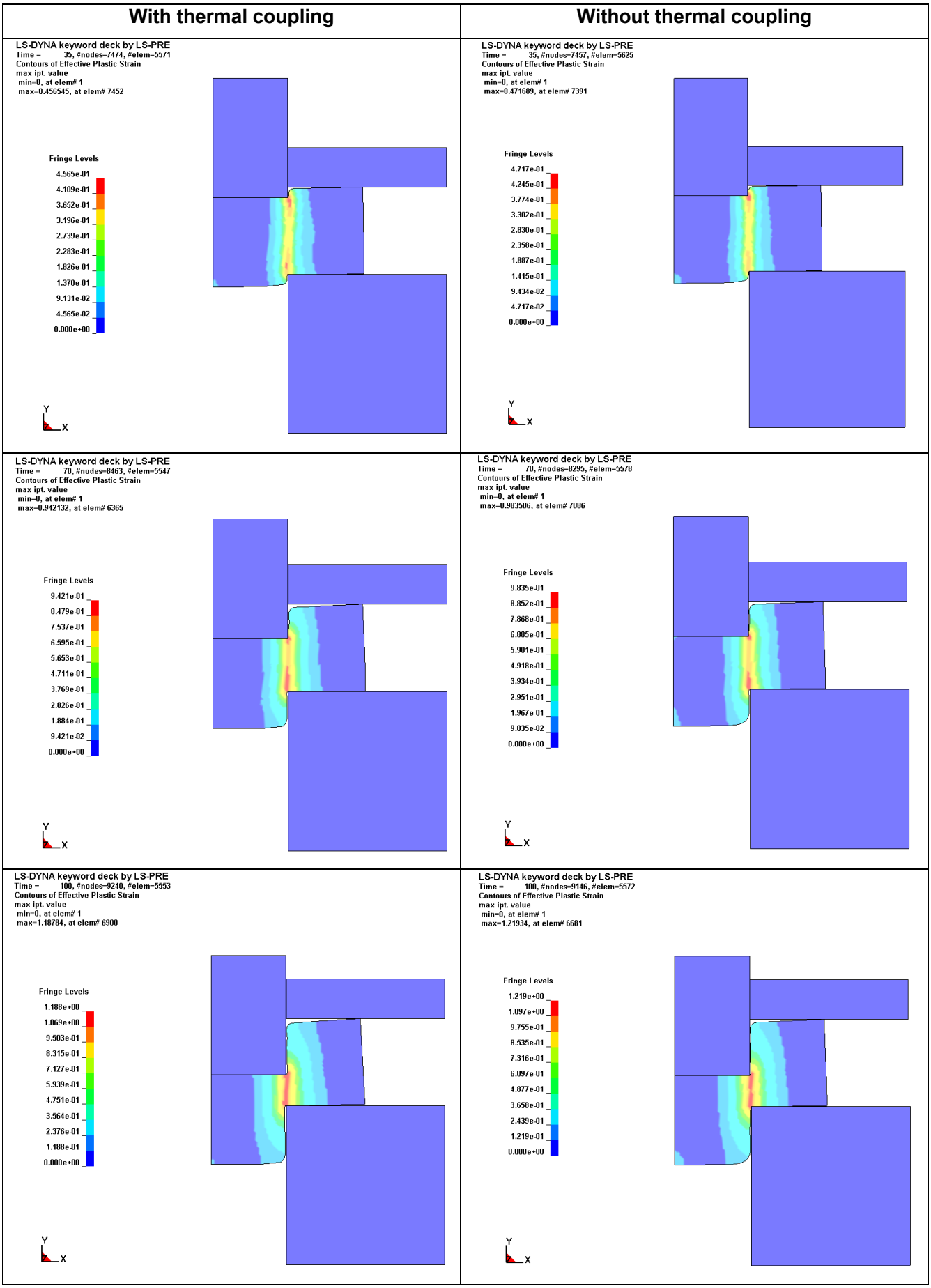


Fig. 13. Punch penetration to metal sheet for a blanking clearance value equal to J1/J2=0.01/0.1mm.

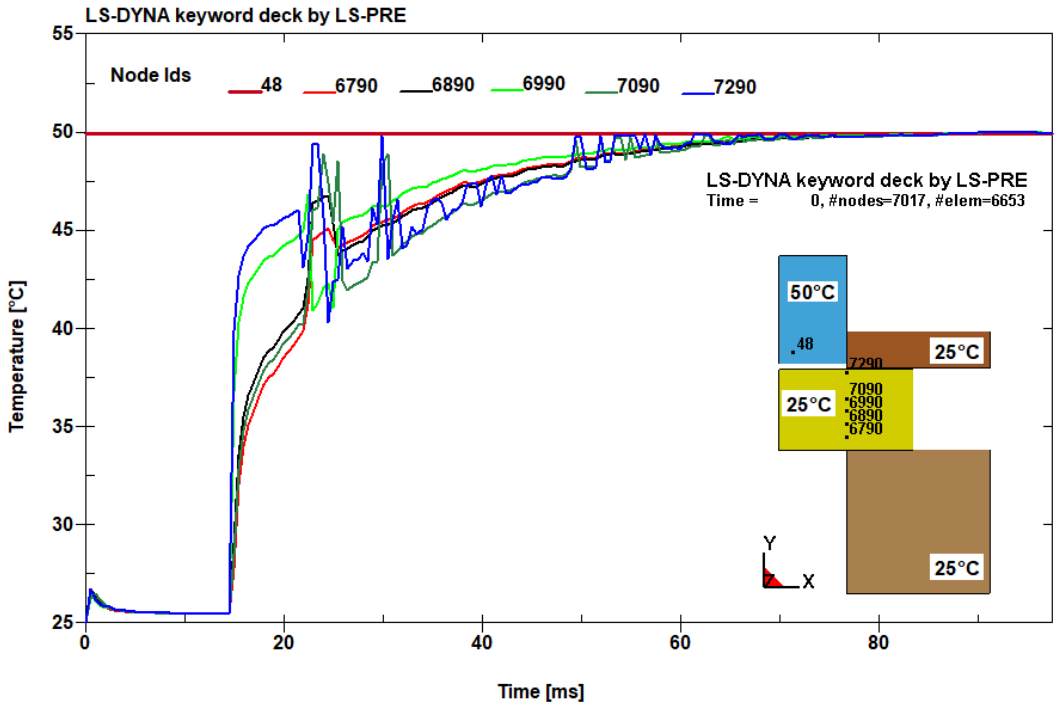


Fig. 14. The temperature evolution in the shear-zone and at the punch surface for an HTC value of 46kW/m^{2}K and an initial punch temperature of 50°C.

Other analyses were conducted, focusing on the effect of punch/die clearance on the profile of the cut part's edge, taking into account, or not, the heating effect of the sheet metal during the cutting process. As illustrated in Fig.16, it was found that the clearance significantly influences the final quality of the cut surface and the final shape of the part (dimensions, burrs, etc.). The estimated values for the three zones of the edge profile, specifically the shear zone, were also sensitive. Indeed, a small punch/die clearance can limit the bending moment acting on the metal part during cutting, due to a small axial displacement between the cutting edges. This bending moment was clearly responsible for the tensile stresses acting in the shear zone. It was therefore evident that the resulting plastic deformations were less significant when the clearance was greater. The literature indicates that tool wear can affect the shear edge, just as the cutting clearance does. On the other hand, the cutting edges become blunt, which promotes the flow of material instead of allowing rapid deformation by shear [36,37].

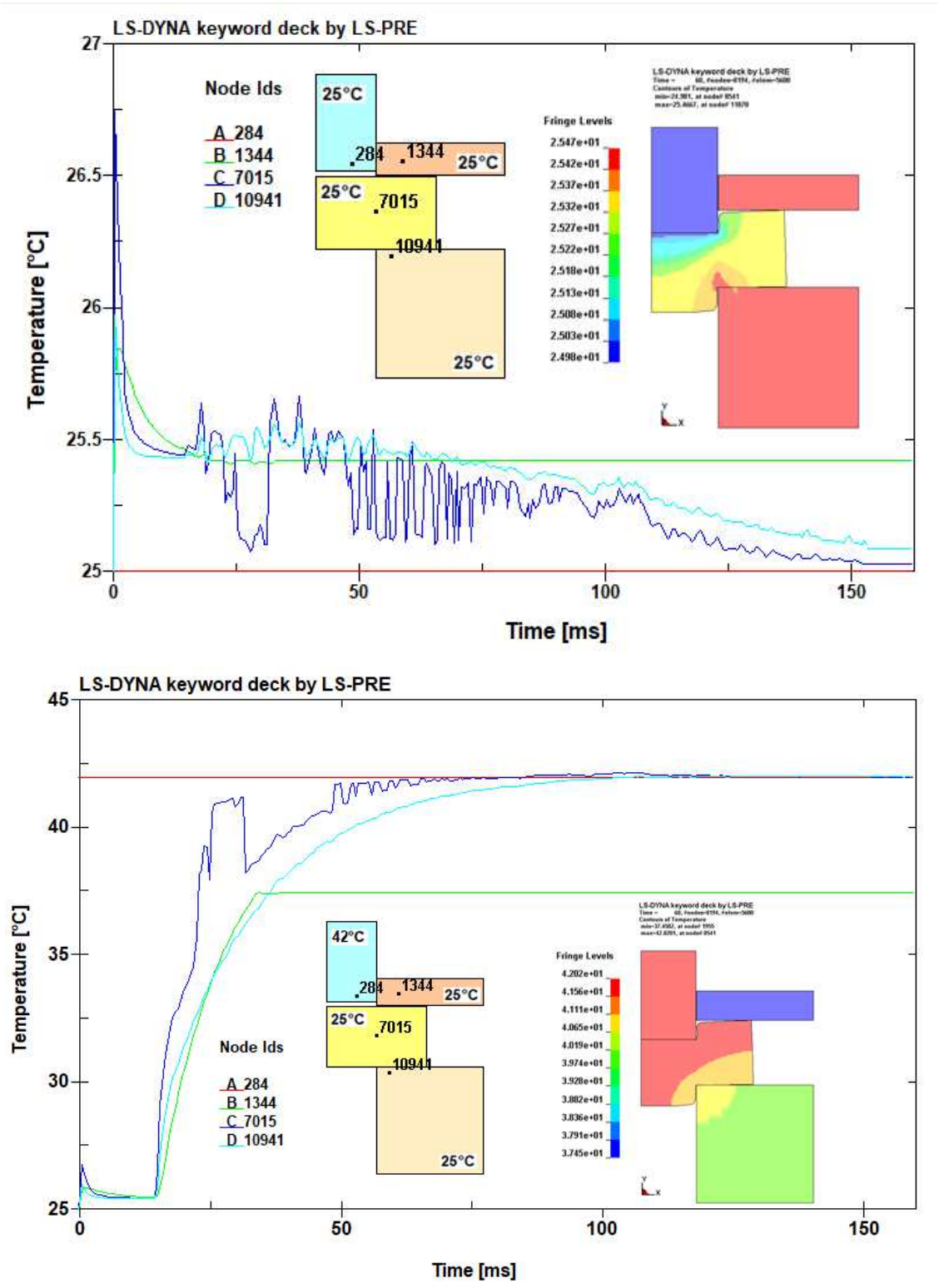


Fig.15. Temperature evolution during blanking process.

Also, in constraints terms, they were high when the punch/die clearance was maximum. These stresses were estimated to be 11-15% less when the sheet metal reached a temperature of 50°C. This temperature was due to the friction of the tools with the material being cut after more than 1500 cycles. This effect can increase tool life.

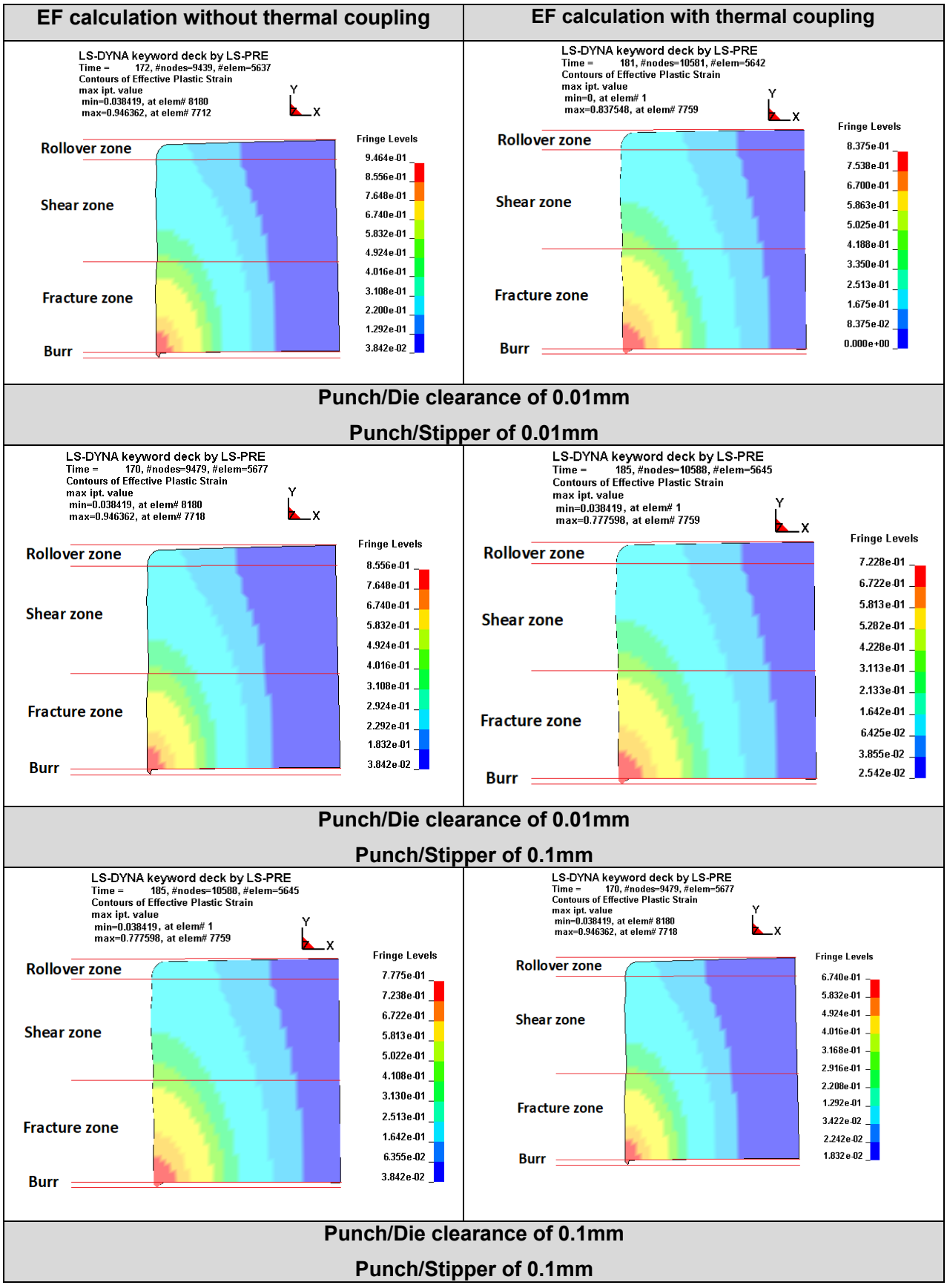


Fig. 16. Sheared edges predicted by FE simulations for different blanking clearances.

Figure 17 presents the results obtained from different simulations of the cutting force as a function of the punch penetration into the sheet metal during a complete cutting cycle, for different punch/die clearance values. The cutting clearances used varied from 0.01 mm to 0.03 mm, as already reported in the previous section 2.2 (see Fig.6). Under the same conditions, the penetration force gradually increases until it reaches a value close to 4.7 kN. It then gradually decreases, slightly faster than the previous step, indicating the initiation of a crack. A low sensitivity to the different punch/die clearance values tested was also observed. Indeed, this penetration force of approximately 4.7 kN decreases slightly and reaches a value close to 4.3 kN when the punch clearance increases. Soares et al. (2013) studied the influence of punch-die clearance (0.2% to 15%) on the quality of punched holes in 8 mm thick sheet metal and on crack propagation. The ideal clearance range for thick ductile materials was between 2% and 10%. However, clearance below 5% can result in lower punching forces. They also observed burrs appearing at clearances of 15% or greater [38].

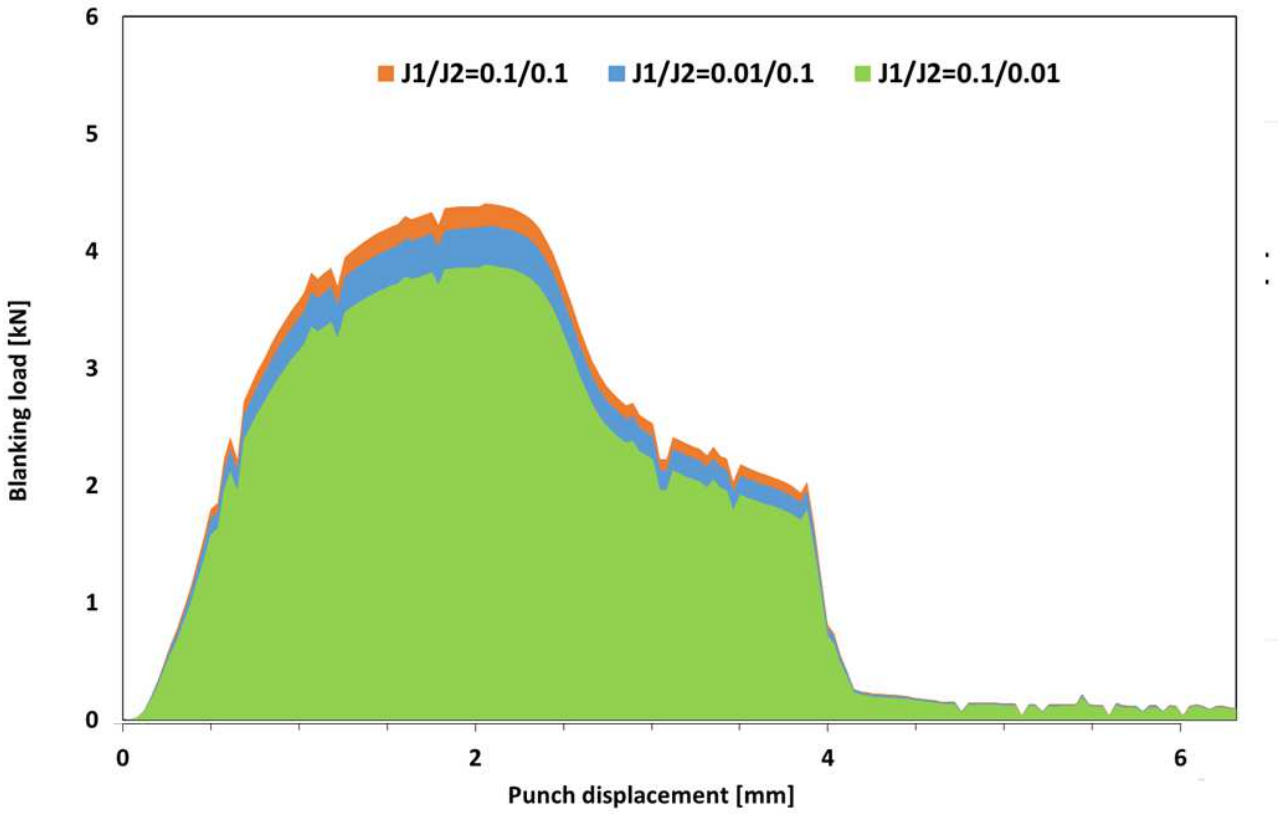


Fig.17. The effect of blanking clearance on the force-displacement curves.

5. Experimental validation

The penetration force of the punch into the sheet metal as a function of the punch displacement was compared to experimental results from our tests on the instrumented tooling. The data were illustrated in Fig.18. It can be clearly seen that the predicted result gets closer and closer to the experimental values as the penetration and/or displacement of the punch increases. It was also noted that the overall error was very low (on the order of 1.3%) for a relatively reasonable computation time (1 hour 17 minutes).

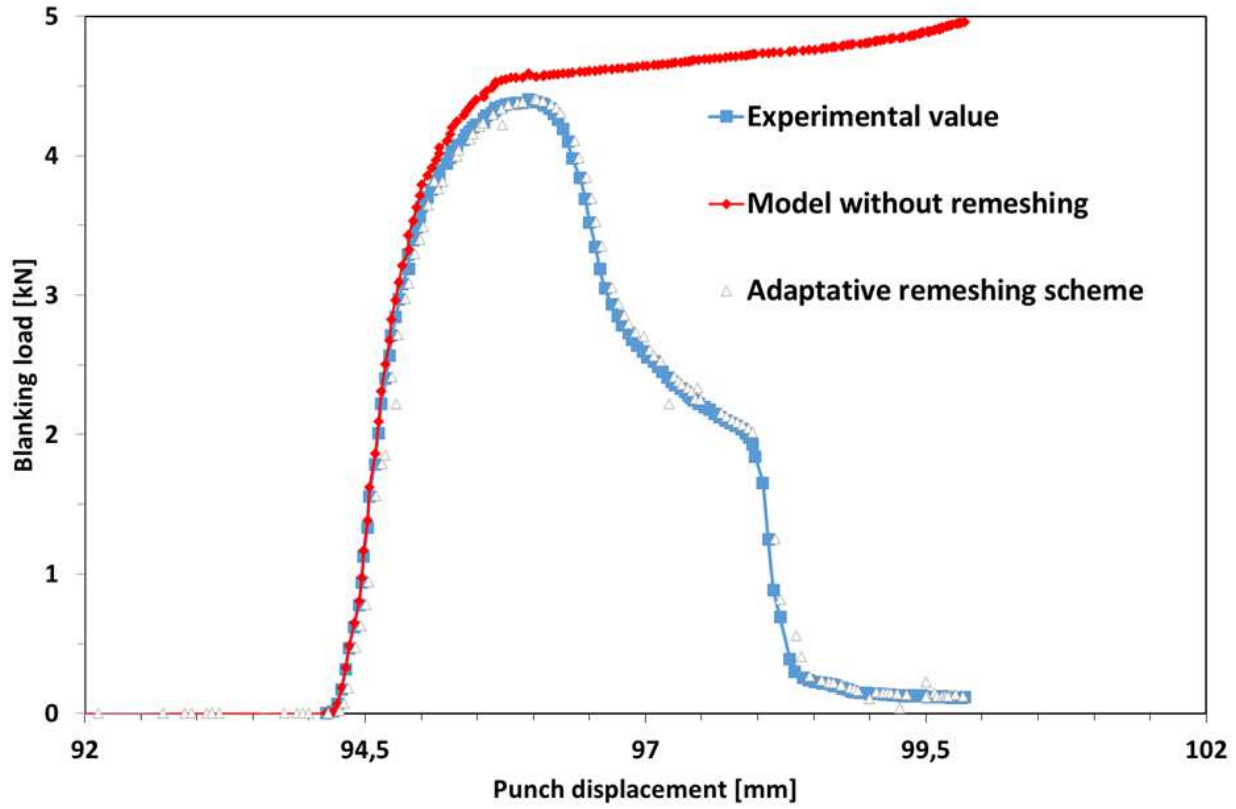


Fig. 18. Predicted blanking force versus punch displacement with and without remeshing.

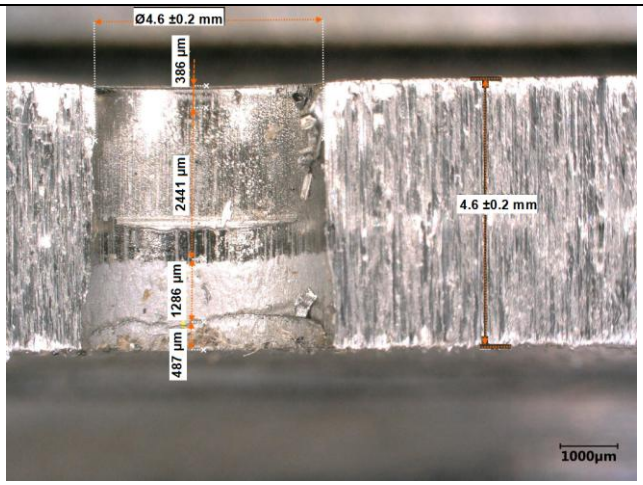
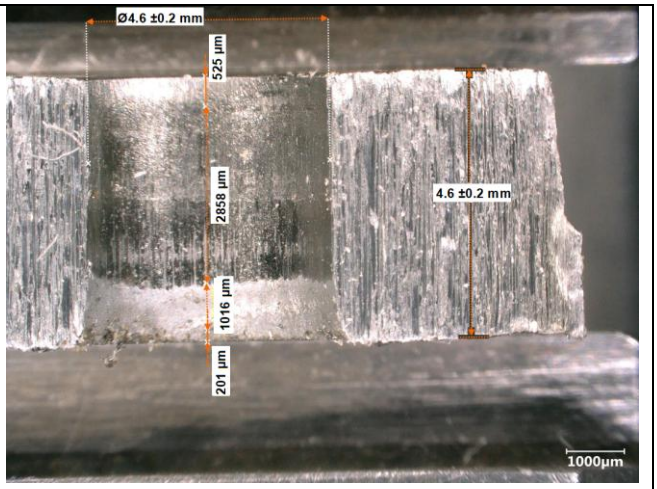
To determine the proportions of fractured and sheared surfaces in the cutting zone, the experimental shear edge was examined under an optical microscope. These measurements were analyzed and then compared to the different shear edges predicted by the FE model.

Comparison of the numerical simulation results with experimental observations reveals a similar distribution of the different shear zones between the simulation and the experiment (Fig.19 and Table 6). Although the absolute values differ, the trends were taken into account to improve the model. The overestimation of the shear zone in our FE model could be explained simply by the phenomenon of elastic return after unloading.

The punch penetration force in the sheet metal as a function of punch displacement during the 50°C cutting test was compared to experimental results from our tests on the instrumented tooling. The data were illustrated in Fig.19. It can be seen that at the beginning

of the blanking process, the experimental/FE simulation error was relatively low, with an error rate close to 1.25%, i.e., the simulated curves show the best agreement with the experimental results. Beyond the maximum cutting force, the observed error increases sharply, with the average error rate reaching 5.37%. The error values for a given cutting displacement were all less than 5%, indicating that good agreement between the simulation and the experimental results was obtained. Indeed, it can be concluded that the numerical simulation was sufficiently accurate to model other scenarios in the blanking process.

The comparison between simulation and experimental results regarding burr height was shown in Fig.19. As expected with significant clearance, the edge profile of the part results in poor quality due to the presence of a large fold and a larger failure zone. This result was consistent with the literature [38-40]. In the simulation, the crack initiates at approximately 30% punch penetration into the sheet metal, while in reality, it initiates at approximately 35.2% penetration. The fold depth was overestimated by our simulations, with a margin of error of approximately 3.1%, because the phenomena of elastic recoil after unloading the punch and the heating of the cutting tool during the various cutting cycles were properly taken into account. Nevertheless, the predicted cutting edge agrees quite well with that obtained experimentally. The simulation results indicate that the shape of the cut part can be predicted. In conclusion, the predictions of the presented EF model agree well with the experimental data.

	
Punch/Die clearance of 0.1µm **Punch/Stipper of 0.01µm**	**Punch/Die clearance of 0.01µm** **Punch/Stipper of 0.01µm**

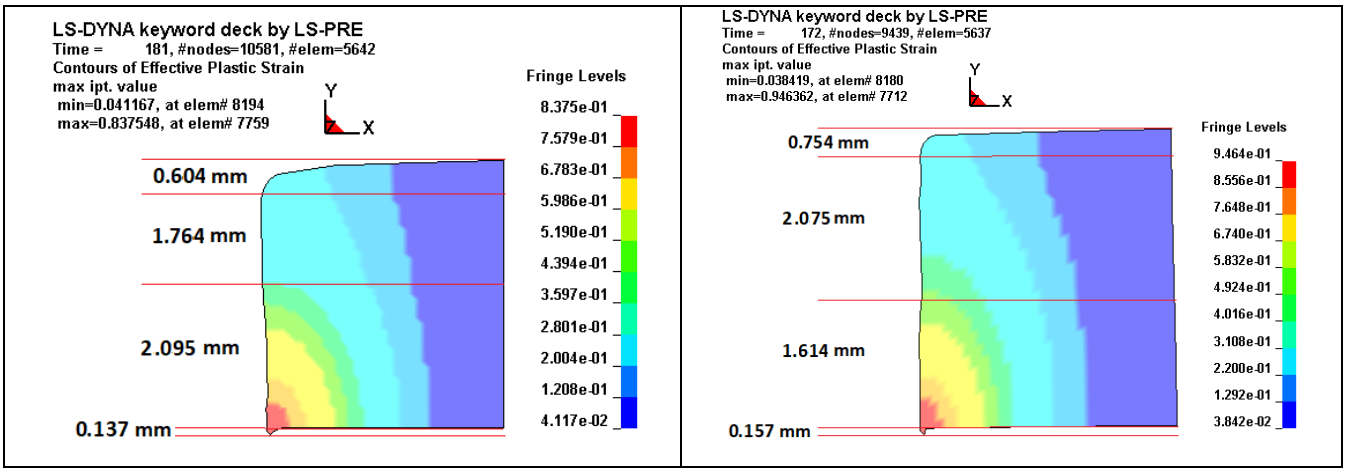


Fig. 19. Characteristic features of sheared edge achieved by optical microscopy analysis and of sheared edge predicted by FE simulations.

The final blanking results were also defined in terms of rollover, burnish, fracture, and burr height, those blanking parameters over the workpiece thickness (see Fig.18). The results were obtained for all three punch/die cutting clearances sets shown in Figure 6 in Section 2.2. The results presented in Table 6 illustrate the average blanking parameters obtained on several workpieces.

6. Conclusions

This article presents a contribution to the numerical simulation of the cold-rolled steel sheet blanking process. The problem was modeled using axial symmetry with the commercial finite element software Lsdyna®. Experimental data allowed the identification of elasto-plastic constitutive law parameters suitable for simulating sheet cutting. The results obtained lead to the following conclusions:

- During numerical simulations of the blanking process, an elongation of the shear surface and a simultaneous reduction of the fracture zone were significantly affected by the punch/die clearance. In general, reducing the clearance delays the initiation of fracture and, consequently, results in a smoother cut surface. However, if the tooling used in the blanking process has a large cutting clearance, it can slightly degrade the quality of the sheared edge.

- Many studies have only reported the maximum temperature values during the different cutting cycles, without detailing the progressive evolution of this

temperature. In our FE model, the temperature evolution of the cut parts, as well as the punch during cutting due to repeated friction, was successfully simulated and taken into account in our calculations to accurately estimate the final profile of the cut edge and the induced stress state. This was made possible by temperature measurements at the point of contact of the punch cutting edge, which accurately predicted ductile fracture and crack initiation.

- The results of the numerical model agree well with experimental results regarding the profiles of the cut edges. However, the FE model was less precise regarding the size of each zone of the cut profile.

Numerical simulation allows us to determine the optimal cutting parameters and proves more economical than using physical prototypes. Further work was needed to incorporate other effects related to the behavior of rolled sheets, such as sheet anisotropy and spring back. In future work, cutting tests will also be extended to higher cutting speeds to further understand sheet behavior and study punch wear.

References

1. W. Zhang, J. Xu, Advanced lightweight materials for automobiles: a review, Mater. Des., 221(27), 110994 (2022).
2. Z. Yang, G. Du, D. Zhao, Z. Luo and Q. Peng , Research on fine blanking strengthening patterns based on 42CrMo steel, Int J Adv Manuf Technol 139, 6009-6016 (2025).
3. R. X. Ding, W. Wang, F. J. Tang, Y. N. Zhou, J. H. Guo, J. H. Duan, L. L. Yan, The effect of crack propagation on the quality of fineblanking surface of cold-rolled steel sheet detected by PVDF film stress sensors. Int J Adv Manuf Technol (99) 1615-1625 (2018).
4. M. Merklein, M. Johannes, M. Lechner, A. Kuppert, A review on tailored blanks – production, applications and evaluation, J. Mater. Process. Technol., (214) 151-164 (2014).
5. H. Mao, S. Li, Y. Liu, L. Hua, An investigation on the microstructure of the fine-blanked sprocket. Int J Adv Manuf Technol (90) 3171-3185 (2017).
6. A. Giampieri, J. Ling-Chin, Z. Ma, A. Smallbone, A.P. Roskilly, A review of the current automotive manufacturing practice from an energy perspective, Appl. Energy, 261 (2020).
7. M.-R. Pendar, F. Rodrigues, J.C. Pascoa, R. Lima, Review of coating and curing processes: evaluation in automotive industry, Phys. Fluids, 34 (2022).

8. C. Lesch, N. Kwiaton, F.B. Klose, Advanced high strength steels (AHSS) for automotive applications – tailored properties by smart microstructural adjustments, Steel Res. Int., 88 (10) (2017).
9. Z. Silvayeh, R. Vallant, C. Sommitsch, B. Götzinger, W. Karner, M. Hartmann, Influence of filler alloy composition and process parameters on the intermetallic layer thickness in single-sided cold metal transfer welding of aluminum-steel blanks, Metall. Mater. Trans., 48A, 5376-5386 (2017).
10. M. Rachik, J.M. Roelandt, A. Maillard, Some phenomenological and computation al aspects of sheet metal blanking simulation. Journal of Materials Processing Technology (128) 256-265 (2002).
11. J. Mucha, An experimental analysis of effects of various material tool's wear on burr during generator sheets blanking, The International Journal of Advanced Manufacturing Technology (50) 495-507 (2010).
12. R. Shivpuri, S. Siddarth, K. Agarwal, C. Liu, Energy release rate-based approach for the wear of punches in precision blanking of high strength steel, CIRP Annals – Manufactoring Technology (60) 307-310 (2011).
13. C. Husson, J.P.M. Correia, L. Daridon, S. Ahzi, Finite element analysis simulations of thin copper sheets blanking: study of blanking parameters on sheared edge quality, Journal of Materials Processing Technology 199,74-83(2008).
14. V. Bratus, F. Kosel, M. Kovac, Determination of optimal cutting-edge geometry on astamped orthotropic circular electrical steel sheet, Journal of Materials Processing Technology 210(2) 396-407 (2010).
15. G-M. Huang, J-P. Wang, T-T. Chen, C-L. Chen and M-H. Xu, Optimal design for the fluid cavity shape in hydromechanical fine blanking, The International Journal of Advanced Manufacturing Technology, (78) 153-160 (2015)
16. Z. Xing, L. Chen, C. Lei, T. Cai, H. Yu, Simulated analysis and experimental investigation on edge qualities of high strength steels hot blanking parts, Procedia Manufacturing, 15 (2018), pp. 619-626
17. J-P. Wang, G-M. Huang, C-C. Chen, Y-C. Ye and T-T. Chen, Investigation of the shear-zone length in fine hydromechanical blanking, The International Journal of Advanced Manufacturing Technology, (68) 2761-2769 (2013)
18. K. Isik, Y. Yoshida, L. Chen, T. Clausmeyer, A. Erman Tekkaya, Modelling of the blanking process of high-carbon steel using Lemaitre damage model, C. R. Mecanique (346) 770-778 (2018).
19. A. Hetzel, M. Merklein, M. Lechner. Enhancement of the Forming Limits for Orbital Formed Tailored Blanks by Local Short-term Heat Treatment. Procedia Manufacturing. (47) 1197-1202 (2020).
20. E. Falconnet, J. Chambert, H. Makich, G. Monteil, Prediction of abrasive punch wear in copper alloy thin sheet blanking, Wear, 338, 144-154 (2015).

21. M. Sahli, X. Roizard, G. Colas, M. Assoul, L. Carpentier, P.H. Cornuault, J.P. Barbe, Modelling and numerical simulation of steel sheet fine blanking process, Procedia Manufacturing, 50, 395-400 (2020).
22. R.K. Pathak, A.R. Kumar, G.K. Ananthasuresh, Simulations and experiments in punching spring-steel devices with sub-millimeter features, J. Manuf. Process., 15 (1), 108-114 (2013).
23. C. Husson, J.P.M. Correia, L. Daridon, S. Ahzi, Finite elements simulations of thin copper sheets blanking: Study of blanking parameters on sheared edge quality, J. Mater. Process. Technol., 199 (1-3) 74-83 (2008).
24. L. Lind, P. Peetsalu, E. Adoberg, R. Veinthal, P. KuluDescription of punch wear mechanism during fine blanking process Proc 7th Int Conf DAAAM Balt Ind Eng, 504-9 (2010).
25. S. Hogmark, K.O. Bengtsson Vingsbo, Wear of steel punches Scand J Metall, 10 (1981).
26. J. J. Hemandez, P. Franco, M. Estrems, F. Faura, Modelling and experimental analysis of the effects of tool wear on form errors in stainless steel blanking. Journal of Materials Processing Technology (180) 143-150 (2006).
27. A.M., L.E. Goijaerts Govaert, F.P.T. Baaijens, Experimental and numerical investigation on the influence of process speed on the blanking process, Journal of Manufacturing Science and Engineering (124) 416-419 (2002).
28. K. Mori, T. Maeno, S. Fuzisaka, Punching of ultra-high strength steel sheets using local resistance heating of shearing zone. Journal of Materials Processing Technology (212) 534-540 (2012).
29. M. Zhang, Study on the thermal blanking of high strength steel based on numerical simulation, Jilin university (2015).
30. X. Peng, X. Lu, R. Balendra, FE simulation of the blanking of electrically heated engineering materials. Journal of Materials Processing Technology (145) 224-232 (2004).
31. P. Sartkulvanich, B. Kroenauer, R. Golle, A. Konieczny, T. Altan, Finite Element Analysis of the Effect of Blanked Edge Quality Upon Stretch Flanging of AHSS. Annals of the CIRP 59, 279–282 (2010).
32. Y. Wang, L. Cao, Z. Bai, et al., A parametric ribcage geometry model accounting for variations among the adult population. J. Biomech. (49) 2791-2798 (2016).
33. G. R. Johnson, & W. A Cook, Constitutive Model And Data For Metals Subjected To Large Strains, High Strain Rates And High Temperatures. (2018).
34. P. Demmel, H. Hoffmann, R. Golle, C. Intra, W. Volk, Interaction of heat generation and material behaviour in sheet metal blanking, CIRP Annals - Manufacturing Technology (2015).

35. A. Rafsanjani, S. Abbasion, A. Farshidianfar, N. Irani, Investigation of the viscous and thermal effects on ductile fracture in sheet metal blanking process. The International Journal of Advanced Manufacturing Technology 45(5-6) 459-469 (2009).
36. F. Gutknecht, F. Steinbach, T. Hammer, T. Clausmeyer, W. Volk, A.E. Tekkaya, Analysis of shear cutting of dual phase steel by application of an advanced damage model, Proc. Struct. Integr. (2) 1700-1707 (2016).
37. J. Stanke, M. Unterberg, D. Trauth, Development of a hybrid DLT cloud architecture for the automated use of finite element simulation as a service for fine blanking, The International Journal of Advanced Manufacturing Technology (108) 11-12 (2020)
38. J. A. Soares, M. L. Gipiela, S. F. Lajarin, P. V. P. Marcondes, Study of the punch–die clearance influence on the sheared edge quality of thick sheets, Int J Adv Manuf Technol (65) 451-457 (2013).
39. E. Taupin, J. Breitling, W-T. Wu, T. Altan, Material fracture and burr formation in blanking results of FEM simulations and comparison with experiments. J Mater Process Technol (59) 68-78 (1996).
40. R. Hambli, Prediction of burr height formation in blanking processes using neural network. Int J Mech Sci (44) 2089-2102 (2002)

Declaration of competing interest

The authors declare that they have no known competing financial interests or personal relationships that could have appeared to influence the work reported in this paper.

The authors declare that no funds, grants, or other support were received during the preparation of this manuscript. The authors have no relevant financial or non-financial interests to disclose.

Author Contributions

All authors contributed to the design and implementation of the study. The preparation of materials, methodology, data collection, testing and characterization, data analysis, writing, review, revision, and supervision were carried out by M. Mohamed Sahli, M. Faleh Rabhi, and Mohamed Abid. The first draft of the manuscript was written by M. Mohamed Sahli and Ms. Rofka Ramdani, and all authors commented on previous versions of this article. M. Mohamed Abid and Ms. Rofka Ramdani performed the formal analysis. All authors read and approved the final version of the manuscript.

Availability of Data and Materials

The experimental and/or numerical data from our simulations in this study are available from the corresponding author upon reasonable request. All materials used in this research, software, and analytical tools are described in detail in the manuscript to ensure reproducibility.